

IMECE2008-67932

EXPERIMENTAL STUDY OF FLUID FLOW IN MICROCHANNEL

Xi Lu and A. G. Agwu Nnanna
 Micro- and Nano-scale Heat Transfer Laboratory
 Department of Mechanical Engineering
 Purdue University Calumet; Hammond, IN 46323-2094
 Tel: (219) 989-2071; Fax: (219) 989-2898;
 Email: nnanna@calumet.purdue.edu

ABSTRACT

This paper presents a study of fluid flow through microchannel. Based on the work of Senta and Nnanna, [23], a trapezoidal-shaped manifold is used to ensure uniform flow distribution in the microchannel. Analysis further shows that flow uniformity among the channels largely depends on shape of the manifolds, length and location of inlet and outlets, and the inlet flow rate. The test setup consists of one hundred twenty-six 14.5 μ m-width channels, flow loop, heat source, thermal sensors and pressure transducers. Flow of fluid through the channels is regulated using a peristaltic pump. Experiments were conducted from various flow rates and heat loads.

According to experimental data, microchannel has significant impact in the heat transfer rate for all the flow rates considered. This enhancement could be attributed to laminar flow in the microchannels, conduction heat transfer through the walls of the channel, fluid-channel wall interaction, and microconvection within the channel. Results show raises some concerns on the use of empirical correlations for flow between two parallel plates to predict heat transfer behavior in microchannels. In the absence of experimental data, $f \approx -2(dp/dx)d_h/\rho u_m^2$ provides a reasonable estimate of friction factor in microchannel.

Keywords: Nanofluid, manifold, microchannel, flow distribution, experiments, numerical, and flow.

NOMENCLATURE

bh base height, m
 d_h hydraulic diameter, m

f	friction factor
ft	fin thickness, m
H	height of channel, m
k _f	thermal conductivity, W/mC
N	number of channels
Nu	Nusselt number
p _o	pressure, N/m ²
q	heat flux, W/m ²
Re	Reynolds number
T _w	base temperature, C
T _m	fluid temperature, C
u _m	velocity, m/s
\dot{V}	volumetric flow rate, m ³ /s
w _c	channel width, m
w	w _c + ft, m

Subscript

c	channel
f	carrier fluid
h	hydraulic
m	mean
w	wall

Symbols

ϵ	porosity of microchannel
ρ	effective density, kg/m ³
ν	effective kinematic viscosity, m ² /s

INTRODUCTION

Fundamental understanding of thermal and hydrodynamic transport phenomena in microchannel is paramount to optimized, efficient and reliable cooling system utilizing micro-heat sinks. Numerous investigations have demonstrated that microchannels have high heat dissipation capability. Tuckerman et

al. [1], in their work on large aspect ratio heat sinks with channel width in the order of 50 μm revealed that power dissipation capability of up to 790 W/cm^2 can be achieved with such a heat sink (with water as coolant), while maintaining the chip temperature rise at only 71°C. In a theoretical study, Philips et al. [2] assessed the performance of microchannel heat sink within the laminar and turbulent regime of hydrodynamically developed or developing flow using a thermal resistance model. They concluded that thermal resistance smaller than 0.1°C cm^2/W can be achieved. Salamm [3] implemented a quasi-two dimensional differential equation to obtain the optimum fin thickness and channel width of the heat sinks. Choquette et al. [4], Sasaki et al. [5], Missaggia et al. [6] and Landram have also done extensive thermal optimization studies for this heat sink. However, it is noted that, their optimum results were normally obtained under a limited geometrical range (for the heat sink) with some parameters fixed on a specific flow and heat transfer regime.

Experimental analysis of the flow and heat transfer characteristics of water flowing through the microchannel made of stainless steel was done by Peng et al. [7]. Their fluid flow results were found to deviate from the values of classical correlation and the transition was observed to occur at the Reynolds number from 200 to 700. These results were contradicted by Xu et al. [8]. Further recent studies confirmed that the behavior of microchannel is quite similar to that of conventional channels. Liu and Garimella et al. [9] showed that conventional correlations offer reliable predictions for laminar flow characteristics in rectangular microchannels over a hydraulic diameter range of 244 – 974 μm .

Little or no experimental work has been performed on thermal/hydrodynamic transport of nanofluid in microchannel. Chein et al. [19] experimentally studied the performance of microchannel heat sink using nanofluids. They found that nanofluid cooled microchannel heat sink (MCHS) could absorb more energy than water-cooled MCHS when the flow rate is low. For high flow rates, the heat transfer was dominated by the volume flow rate and nanoparticles did not contribute to the extra heat absorption. Their measured MCHS wall temperature variations agreed with the theoretical prediction for low flow rate. For high flow rate, the measured MCHS wall temperatures did not completely agree with the theoretical prediction due to the particle agglomeration and deposition. In a numerical investigation of cooling performance of a microchannel heat sink with nanofluids (6nm copper-in-water and 2nm diamond-in-water), Jang et al. [20] concluded that the cooling performance of water-

based nanofluids containing diamond (1 vol. %, 2 nm) at the fixed pumping power of 2.25W is enhanced by about 10% compared with that of a microchannel heat sink with water. Also, that nanofluid reduces both the thermal resistance and the temperature difference between the heated microchannel wall and the coolant. Chein et al. [21] in their work on analysis of microchannel heat sink performance using nanofluids, they concluded that no additional penalty in pressure drop is incurred by using nanofluid as the coolant.

Review of literature shows that nanofluid/micro-channel heat sinks have high heat dissipation capability, low thermal resistance, and could potentially be the next generation cooling system. However, the deposition of nanoparticle on the channel wall, interaction between particle and the channel walls have not been fully assessed. If the particles deposit on the walls, this could increase the wall thermal resistance in a replica manner to fouling in pipe walls. In addition, the relationship between channel aspect ratio and volume fraction, changes, if any, in thermophysical properties of nanofluid at the exit of the channel has not been appraised. This information is consequential to the comprehension of nanofluid transport behavior in microchannels. The objectives of this study are to experimentally investigate the hydrodynamic interactions of nanoparticles in microchannel, and the impact of pressure drop and nanoparticle concentration on thermal augmentation, and finally to estimate the optimum volume fraction, flow rate, and pressure drop that result in maximum heat transfer rate.

MATHEMATICAL FORMULATION

Figure 1 presents a schematic of the microchannel heat sink. According to Ref. [21], assuming uniform heat distribution on the bottom of the heat sink, and that the fluid flows uniformly across each channel, the velocity and hydraulic diameter, d_h can be respectively expressed as

$$u_m = \frac{\dot{V}}{NHw_c} \quad (1)$$

$$d_h = \frac{2Hw_c}{H + w_c} \quad (2)$$

where \dot{V} is the volumetric flow rate, N is the number of channels, H is the height, and w_c is the channel width. The Reynolds number is $\text{Re} = u_m d_h / \nu$, where ν is kinematic viscosity.

Based on the value of the Re, it is determined whether the flow is hydrodynamically and/or thermally developed, using expressions from [23]

$$(x_{fd,t})_{lam} = 0.05d_h Re_{dh} Pr \quad (3)$$

$$(x_{fd,h})_{lam} = 0.05d_h Re_{dh} \quad (4)$$

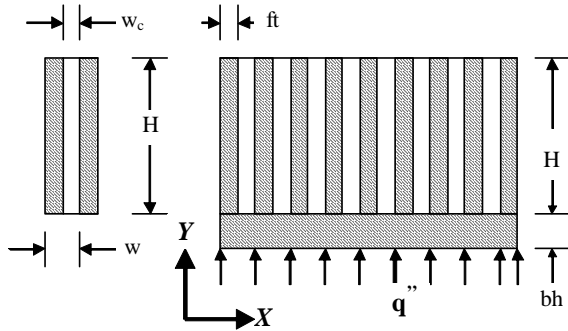


Figure 1. Schematic of heat sink microchannel

The Nusselt number is expressed as

$$Nu_o = \frac{2q_w''H}{\varepsilon k_f (T_w - T_m)} = \frac{2Hh_m}{\varepsilon k_f} \quad (5)$$

where $\varepsilon = w_c/w$ is the porosity of the microchannel heat sink, and $w = w_c + ft$. Based on the experimentally measured data in this work, the friction factor [23] is computed using

$$f \approx \frac{-2(dp/dx)d_h}{\rho u_m^2} \quad (6)$$

Equation (6) will be compared with $f = \frac{64}{Re_{dh}}$ to ascertain the deviation of the flow regime from the classical equation for friction factor in laminar flow.

EXPERIMENTS

For brevity, details of the manifold design will not be discussed in this paper and can be found in Senta and Nnanna, [23]. The key consideration in the design of the jacket (manifold) is to ensure uniform distribution of fluid in all the channels, thereby minimizing dead volumes and hot spots. Several jacket shapes such as rectangular, trapezoidal, square, etc, and fluid inlet and exit locations were considered. Numerical studies were performed to investigate the best shape for inlet/outlet manifold designs. Using Fluent, Computational Fluid Dynamics software, the geometries were designed, meshed, and appropriate boundary conditions were assigned. For each of the geometries, attention were given to performance criteria such as the nature of the fluid distribution, accumulation of large dead volume at the corners, back flow, excess pressure drop if more than one inlet

is allocated in the design etc. So these initial numerical outputs led to the refining and iteration of designs until an optimum design is obtained. Based on comparison of the performance criteria for each of the geometries, result shows that the trapezoidal shaped manifold, see Fig. 2, yields the “best” flow distribution and that flow uniformity among the channels largely depends on the shape of the manifolds, length and location of inlet and outlets.

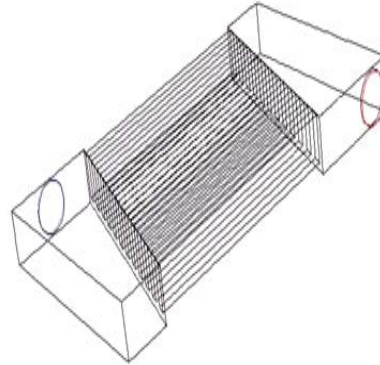


Figure 2 Trapezoidal manifolds with circular-shaped inlet and open outlet

The test setup is depicted in Figs. 3a and 3b. It consists of deionized water, micro pumps, flow meter, pressure transducers, and microchannel test section, hollow jacket consisting of inlet/outlet manifolds, micro condenser and data acquisition system. The microchannel heat sink is donated by Fujikura Ltd, Japan. It has 126 microchannels fabricated using copper material, and a footprint area of $24.76\text{mm} \times 24.76\text{mm}$. The channel width and height is $14.5\mu\text{m}$ and 4.8mm , respectively.

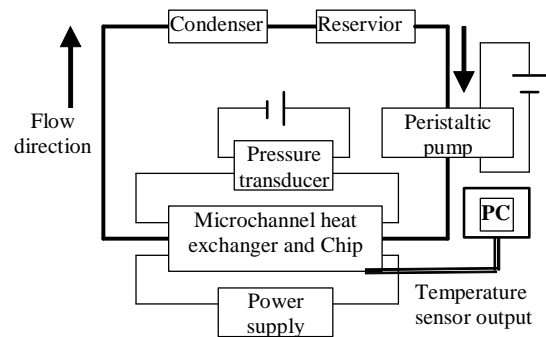


Figure 3a. Schematic of experimental setup

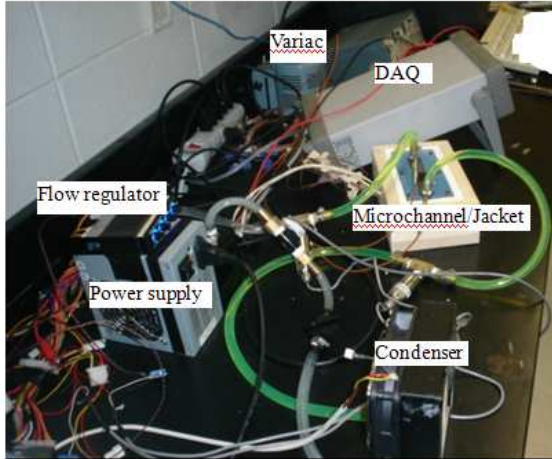


Figure 3b. Experimental facility

The condenser is a 1-shell and 2-tube pass heat exchanger. Fluid is propelled through the condenser using a bidirectional, self-priming peristaltic pump for precise low flow deliveries. The flow is proportional to the speed of the pump head and the inside diameter of the tubing, both of which can be varied. It has a variable speed flow control and five different sized tubing assemblies to provide fine resolution with a wide range of flow rates.

The heat source is a 2.5cm × 2.5cm foot-print area aluminum block with four through-holes drilled along the length of the aluminum block for placement of heater cartridges. A total of four cartridges were used. Each generates a maximum of 150 Watts hence the maximum heat output is 450 Watts. The cartridges are electrically connected in parallel to each other to maintain a constant voltage across the heaters and also to increase power output. All the cartridges are connected to a power supply which controls the voltage and current output from the heater.

To study the heat transfer behavior across the microchannel, thirty-two type-T thermocouples were attached at pre-selected sites to monitor the variation of fluid temperature, base and wall temperature of the microchannel heat sink. Differential pressure transducers are installed at the inlet and the outlet of the heat sink test section. The pressure transducers are temperature sensitive and adjust according to the variation of the fluid inlet and exit temperature.

All the thermocouple and pressure transducer wires were connected to three twenty-channel Reed plug-in module with a built-in temperature compensation for direct temperature measurement. Each module has twenty channels and communicates with the floating logic via the internal isolated digital bus of the data logger HP34970A. Temperature and pressure measurements from the data logger are

automatically recorded in the personal computer for further data reduction.

As depicted in Fig. 3, all the components are connected to each other via a piping network. The pipe is a silicon-based flexible pipe, a control valve attached to the pipe is used to regulate the nanofluid flow rate. In addition to the valve, the rate of flow is also controlled using the built-in meter on the peristaltic pump. This help in providing flow in the range of ultra flow, low ultra flow and also to medium flow. Once the test section is assembled, the pump attached to the reservoir is activated to charge the system with nanofluid and consequently degasify the components.

The microchannel test piece is mounted on the trapezoidal jacket and a water-proof sealant along with a gasket is applied between the mating surfaces to avoid leakage and contamination (dust particles, dust vapors etc).

The heater power supply is switched on and maintained at the required power level, and a steady state is reached. As the test section is heated and the nanofluid is allowed to flow through the channels, readings for temperature variation are collected from all the thermocouple attached to the test section. All the temperature data's from the thermocouple are stored in the data acquisition system throughout the duration of the experiments. The steady state values are calculated on the average of all the reading recorded during that span of time.

The main source of uncertainties is error due to the measurement of temperature, heat transfer rate, and physical dimensions. The combined uncertainty of the data logger HP34970A and the thermocouple calibration in the measurement of temperature is ±0.4% or ±0.5°C, whichever is greater. The error associated with heat transfer rate is due to voltage and current measurements, and are respectively, ($U_v = 0.05\%$ of setting + 90mV) and ($U_I = 0.1\%$ of settling +35mA), [22]. The combined uncertainty of the current and voltage in the heat transfer rate is expressed as

$$U_q = \sqrt{(U_I \partial q / \partial I)^2 + (U_V \partial q / \partial V)^2}$$

RESULTS AND DISCUSSIONS

Temperature data measured along the base of the microchannel/jacket is presented in Fig. 4 for applied power of 100W. Each curve represents a volumetric flow rate. A total of twelve flow rate were tested ranging from 10LPH to 400LPH. The maximum temperature occurred at the mid-point of the heat source. Data from Fig. 4 shows non-uniformity in base temperature distribution, thermal spreading

resistance, and that the 400LPH flow rate has the lowest base temperature.

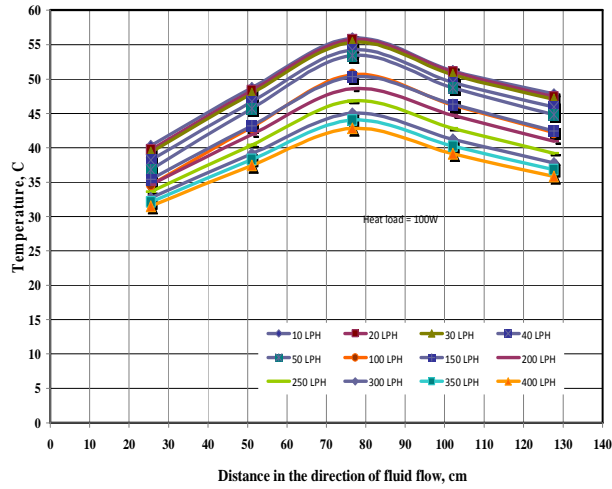


Figure 4. Base temperature distribution

Figures 5 and 6 compare the heat source temperature for fluid flow, with and without the microchannel. According to data from Fig. 5, microchannel has significant impact in the heat transfer rate for all the flow rates considered. A temperature difference of about 23°C is observed. This enhancement could be attributed to laminar flow in the microchannels, conduction heat transfer through the walls of the channel, fluid-channel wall interaction, and microconvection within the channel. Presently, additional work is being conducted to better understand the thermal augmentation due to microchannel.

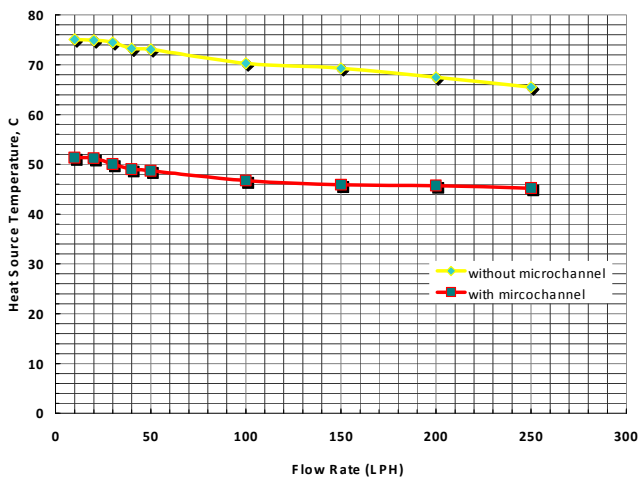


Figure 5. Comparison of heat source temperature, with and without microchannel for various flow rates

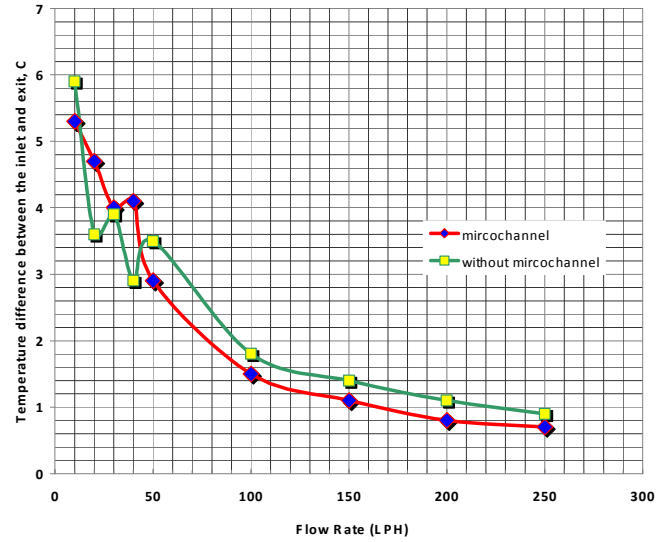


Figure 6. Comparison of inlet and exit flow temperatures, with and without microchannel for various flow rates

In an effort to study the impact of microchannel on flow field and heat transfer, a preliminary test of fluid flow through the manifold without the microchannel was performed, and the result is presented in Fig. 7 as the variation of Nusselt number with Reynolds number. The Nusselt number is expressed in Eq. (5) as $Nu = q''L/k\Delta T$. It should be pointed out that three Reynolds number are in the test setup: Re-value in the pipe that carries fluid into the manifold, Re-value in the manifold, and Re-value in the microchannel. The Re-values plotted in Fig. 7 refers to those within the manifold. Figure 7 reveals an increase in Nusselt number with Reynolds number for various flow rates.

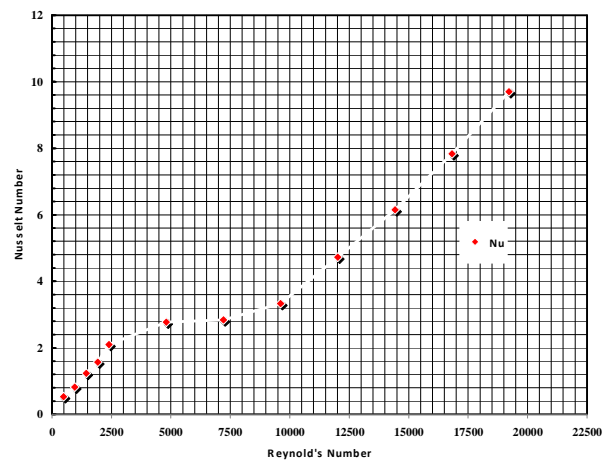


Figure 7. Nusselt number as a function Reynolds number without microchannel

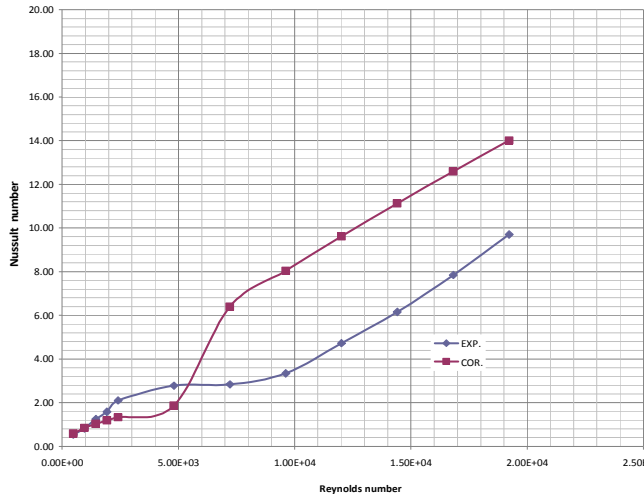


Figure 8. Nu as a function of Re with microchannel

Nusselt number correlations for flow between parallel plates are expressed in [23] as $Nu = 0.335Re^{1/2} Pr^{1/2}$ and $Nu = 0.36Re^{4/5} Pr^{3/4}$ for laminar and turbulent flow, respectively. Using these correlations, the Nu is calculated and compared with experimentally determined Nu as shown in Fig. 8. It reveals significant discrepancy between the experimental and Nu correlations especially in the turbulent region. This raises concern on the approximation of microchannel flow as fluid flow between parallel plates.

The inlet and exit pressure across the microchannel for various flow rates is plotted in Fig. 9. The maximum pressure drop is 24KPa. Equation (6), $f \approx -2(dp/dx)d_h/\rho u_m^2$ is plotted in Fig. 10 as a function Re. It is observed that the friction fraction decreased with Reynolds number.

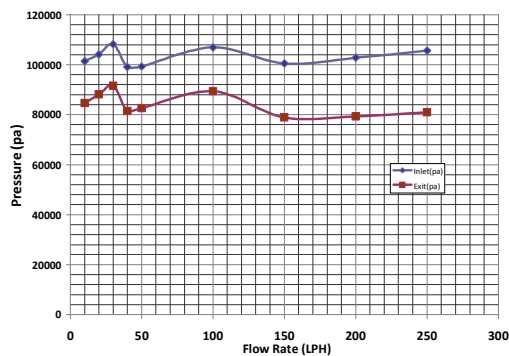


Figure 9. Variation of pressure drop with flow rate

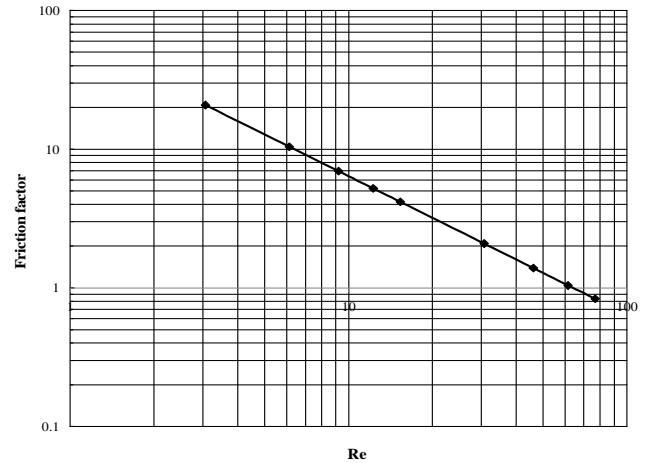


Figure 10. Friction factor as a function of Re

SUMMARY

An experimental study of fluid flow through microchannel has been performed. Based on the work of Senta and Nnanna, [23], a trapezoidal-shaped manifold is used to ensure uniform flow distribution in the microchannel. Analysis further shows that flow uniformity among the channels largely depends on shape of the manifolds, length and location of inlet and outlets, and the inlet flow rate.

The test setup consists of one hundred twenty-six 14.5 μ m-width channels, flow loop, heat source, thermal sensors and pressure transducers. Flow of fluid through the channels is regulated using a peristaltic pump. Experiments were conducted from various flow rates and heat loads.

According to experimental data, microchannel has significant impact in the heat transfer rate for all the flow rates considered. This enhancement could be attributed to laminar flow in the microchannels, conduction heat transfer through the walls of the channel, fluid-channel wall interaction, and microconvection within the channel. Results show raises some concerns on the use of empirical correlations for flow between two parallel plates to predict heat transfer behavior in microchannels. In the absence of experimental data, $f \approx -2(dp/dx)d_h/\rho u_m^2$ provides a reasonable estimate of friction factor in microchannel.

REFERENCES

1. D. B. Tuckerman and R. E W. Pease, 1981, "High performance heat sinking for VLSI," IEEE Electronic Device Letters, vol. EDL-2, no. 4, pp 126-129.
2. R. J. Phillips, "Microchannel heat sinks", Advances in thermal modeling of electronic

- components and systems, (Edited by A. Bar-Cohen and A. D. Kraus), pp 109-184, ASME, New York, 1990.
3. V. J. Salman, 1989, "Convective Heat Transfer in Microchannels," *Journal of Electronic Materials*, Vol. 18, No.5, pp 611-618.
 4. S. E Choquette, M. Faghri, 1996, "Optimum design of microchannel heat sinks," *MEMS, ASME DSC-Vol.59*, pp. 115-126.
 5. S. Sasaki and T. Kishimoto, 1986, "Optimal Structure for Microgrooved Cooling Fin for High-powered LSI Devices," Vol. 22, No. 25, pp. 1332-1334.
 6. L. J. Missaggia, J. N. Walpole, Z. L. Liau and R. J. Phillips, 1989, "Microchannel Heat Sinks for 2-D High Power Density Diode Laser Arrays," *BEE Journal of Quantum Electronics*, QE 25, No. 9, pp 1988-1992.
 7. X. F. Peng, G. P. Peterson, B. X. Wang, 1994, "Heat Transfer Characteristics of Water Flowing through Microchannels," *Exp. Heat Transfer* Vol. 7, pp. 265-283.
 8. B. Xu, K. T. Ooi, N. T. Wong, W. K. Choi, 2000, "Experimental Investigation of Flow Friction for Liquid Flow in Microchannels," *Int. Comm. Heat Transfer*, Vol. 27, pp. 1165-1176.
 9. D. Liu, S. V. Garimella, 2000, "Investigation of Liquid Flow in Microchannels," *AIAA J. Thermophys. Heat Transfer*, Vol. 18 pp. 65-72.
 10. Wang, X., Xu X., and Choi, U. S., 1999, "Thermal Conductivity of Nanoparticle-Fluid mixture," *Journal of Thermophysics and Heat Transfer*, 13(4), pp. 474-480.
 11. Amiri, A. and Vafai, K., 1994, "Analysis of Dispersion Effects and Non-thermal Equilibrium, Non-Darcian, Variable Porosity Incompressible Flow through Porous Media," *International Journal of Heat and Mass Transfer* Vol. 37, pp. 939-954.
 12. Amiri, A. and Vafai, K., 1998, "Transient Analysis of Incompressible Flowthrough a Packed Bed," *International Journal of Heat and mass Transfer*, Vol. 41, pp. 4259-4279.
 13. Bear, J., 1972, *Dynamics of Fluids in Porous Media*, Dover Publications, New York.
 14. Kaviany, M., 1991, *Principles of Heat Transfer in Porous Media*, Springer-Verlag, New York.
 15. Nield, D. A. and Bejan, A., 1992, *Convection in Porous Media*, Springer, New York.
 16. Eastman, J. A., Choi, S. U. S., Li S., Soyez, G., Thompson, L. J., and Melfi, Di, 1999, "Novel Thermal Properties of NanoStructured Materials," *Materials Science Forum*, Vol. 312-314, pp. 629-634.
 17. Lee, S., and Choi, S. U. S., 1996, "Application of Metallic Nanoparticle Suspensions in Advanced Cooling Systems," *ASME Recent Advances in Solids/Structures and Application of Metallic materials*, PVP-Vol. 342/MD-Vol. 72, pp. 227-234
 18. Xuan, Y., and Roetzel, W., 2000, "Conceptions for heat Transfer Correlation of Nanofluids," *International Journal of Heat and Mass Transfer*, Vol. 43, pp. 3701-3707.
 19. R. Chein and J. Chuang, 2007, "Experimental Microchannel Heat Sink Performance Studies using Nanofluids," *International Journal of Thermal Sciences*, Vol. 46, Issue 1, pp. 57-66
 20. S. Jang, S. U. S. Choi, 2006, "Cooling Performance of a Microchannel Heat Sink with Nanofluids," *Applied Thermal Engineering*, Vol. 26, pp. 2457-2463.
 21. R. Chein, and G. Huang, 2005, "Analysis of Microchannel Heat Sink Performance using Nanofluids," *Applied Thermal Engineering*, Vol. 25, pp. 3104-3114.
 22. A. G. A. Nnanna, 2007, "Experimental Model of Temperature-Driven Nanofluid," *Journal of Heat Transfer*, Vol. 129 (6), pp. 697-704.
 23. M. Senta and A. G. Agwu Nnanna, 2007, "Design of Manifold for Nanofluid Flow in Microchannels," *Proceedings of the ASME Int. Mechanical Engineering Congress and Exposition*, No. IMECE2007-42720, pp. 1-8, November 11-15, 2007, Seattle, Washington
 24. F. P. Incropera and D. P. Dewitt, 1990, *Fundamental of Heat and Mass Transfer*, 3rd Ed. John Wiley & Sons, Inc., New York.